ELSEVIER

Journal of Alloys and Compounds 434–435 (2007) 559–564

Journal of ALLOYS AND COMPOUNDS

www.elsevier.com/locate/jallcom

An atomistic study of mechanical deformation of nanostructured Ni_3Al synthesized by cluster compaction

Evgeny E. Zhurkin [a,b], Marc Hou [a,*]

[a] *Physique des Solides Irradiés et des Nanostructures CP234, Universitè Libre de Bruxelles, boulevard du Triomphe, 1050 Brussels, Belgium*

[b] *Department of Experimental Nuclear Physics K-89, St. Petersburg State Polytechnical University, 29 Polytekhnicheskaya street, 195251 St. Petersburg, Russia*

Available online 28 September 2006

Abstract

The mechanical deformation properties of nanostructured Ni_3Al under uniaxial tensile load were studied at the atomic scale by computer modeling. The simulations were performed using a classical Molecular-Dynamics scheme based on combined Rahman–Parinello and Nosé techniques with a many body interatomic potential. This potential is designed in the frame of the second moment approximation of the tight-binding model. A model sample was prepared by simulation of the compaction of isolated Ni_3Al clusters with diameters in the range of 3.3–6.4 nm under 2 GPa external hydrostatic pressure at room temperature. After this model treatment, clusters were found to keep their identities, and their structure and segregation state did not differ much from those in the initial free clusters. Then, a uniaxial tensile stress was applied, and the strain evolution was followed as a function of time at different constant temperatures. The presence of both elastic and plastic regimes of deformation was observed, depending on the magnitude of the applied load. The Young modulus, the Poisson ratio and the elastic limit were estimated as functions of temperature. The possible intra- and inter-granular plastic deformation mechanisms are briefly discussed.

Keywords: Clusters; Nanostructures; Nanofabrications; Strain; High pressure; Elasticity; Atomic scale modeling

1. Introduction

The possibility to synthesize nanostructured materials (NsM) gives the hope to obtain original mechanical properties, like for instance, superplasticity in metals and alloys at low temperatures [1]. NsM are characterized by a large amount of grain boundaries and their influence on plasticity may be significant. In coarse-grain samples, interfaces represent obstacles to the deformation processes that results in hardening associated to dislocation pile up. In NsM however, experimental evidence was found for the absence of dislocation pile up during mechanical deformation [2] and, to a large extent, interfaces are expected responsible for the observed plasticity. In coarse-grained polycrystalline materials, the plastic deformations result to a large extent from dislocation activity and grain boundary junctions instability. However, in NsM (with grain size typically less than 100 nm), due to the large volume fraction occupied by interfaces as compared to polycrystals, the role of interfaces is expected to be crucial. If the NsM is formed by grains with sizes smaller than about 10 nm, no dislocation activity is expected [3] and the role of interfaces and interface junctions in mechanical properties may become dominant. Interfacial diffusion is predicted very high and diffusion coefficients were predicted as high as in a liquid [4,5]. Several mechanisms of deformation (like GB sliding, grain rotation, interfacial viscosity, etc.) have been discussed [3]. Such grains contain no more than several thousands of atoms, in contrast to normal polycrystals (with typical grain size about a few micrometers). The latter grains are too large for modeling by atomic scale simulation techniques). In NsM a collection of grains forming a nanostructure can realistically be modelled at atomic level at the 1:1 scale on currently available Parallel Computer Systems. Hence, it is possible to reproduce at atomic scale most of possible deformation mechanisms in NsM. However, time scale limitations (typically in the nanoseconds range) make it impossible to reproduce experimental strain rates. Therefore, atomic scale simulations can only model the initial stage of deformation which, however, already includes collective motion such as GB sliding and dislocation nucleation at GBs. Several works were devoted to study of mechanical properties of NsM

* Corresponding author. Tel.: +32 2 650 5735; fax: +32 2 650 5227.
E-mail addresses: ezhurkin@phmf.spbstu.ru (E.E. Zhurkin), mhou@ulb.ac.be (M. Hou).

0925-8388/$ – see front matter © 2006 Elsevier B.V. All rights reserved.
doi:10.1016/j.jallcom.2006.08.183

at the atomic scale [3,6–8]. Simulated nanostructured materials may be constructed in different ways mimicking experimental preparation methods. Two basic groups of NsM preparation techniques may be mentioned: one step methods and two step methods. One step methods (as electrodeposition or severe plastic deformation) result in dense compact materials. The atomic scale structure of such materials is modelled, for instance, by Voronoi construction, starting from randomly distributed and oriented seeds (see, for instance, Ref. [8]). Nanostructured solids can also be synthesized in two steps (e.g., by inert gas condensation followed by compaction [9] or nanocluster synthesis followed by low energy cluster beam deposition (LECBD) [10]). Produced in such ways, NsM materials contain voids and they may therefore have significantly lower densities than polycrystalline or single crystal solids. These voids may play a role in plastic deformation which is specific to cluster assembled materials (CAM). The atomic scale modeling of the synthesis of such materials can also be achieved at the atomic scale (see, for instance, Refs. [11–14]).

In what follows, the model synthesis of Ni_3Al nanostructured materials by cluster assembling and compaction is briefly outlined and the mechanical response of the model sample to a uniaxial load at various temperatures is characterized.

2. The method

2.1. The interatomic potential

In order to describe equilibrium properties of metals and their alloys correctly, it is necessary to use a many body potential. The total energy of a system is given by:

$$E_{\mathrm{coh}} = \frac{1}{2}\sum_{i\neq j} V_{ij}(x) - \sum_{i} F_i(x) \tag{1}$$

where $x = |\boldsymbol{r}_i - \boldsymbol{r}_j|$ is the interatomic distance between two atoms i and j, V_{ij} is a repulsive pair potential while F_i is associated with an attraction due to the local electronic density or the band bonding. We select a potential based on the second moment approximation of the tight-binding model using cubic splines which is proposed by Ackland and Vitek [15,16], where $F_i = (\sum \Phi_{ij}(x))^{1/2}$ and $\sum \Phi_{ij}(x)$ is a superposition of local electronic densities over all bonds with neighbors of an atom i. The range of the local interaction is limited by a cut-off distance taken in Refs. [15,16] as $1.225a_0$, where a_0 is the lattice parameter. This is the same potential as used in the study isolated Ni–Al and Cu–Au clusters and bulk alloys presented in Refs. [13,17,18]. The parameters suggested by Gao, Bacon and Ackland [19] were checked to allow an excellent prediction of the elastic constants of Ni_3Al as well as of the cohesive energy and equilibrium lattice parameter of Ni_3Al. These were used in the present work.

2.2. The atomic scale models

In this section, we briefly describe the atomic scale methods used to model free clusters, their compaction into a nanostructured material end the mechanical deformation induced by a uniaxial stress.

Equilibrium Ni_3Al clusters are modeled by importance sampling according to the Metropolis Monte-Carlo method, which is well described, among other, in Ref. [20]. The problem we have to deal with involves thermal vibrations, the relaxation of highly and inhomogeneously stressed systems, and segregation. The segregation process involves high energy barriers as well as complex diffusion jumps that are rare events. Therefore, rather than considering the physical path to equilibrium, we employ the MMC method in the statistical ensemble currently called "semi-grand canonical ensemble" ($\Delta\mu$-NPT) [21]. For the purposes of our study, allowing for transmutations make the algorithm particularly efficient for predicting segregation. In this approach, the temperature (T), the pressure (P), the chemical potentials difference ($\Delta\mu = \mu_{\mathrm{Al}} - \mu_{\mathrm{Ni}}$) and the total number of particles ($N = N_{\mathrm{Al}} + N_{\mathrm{Ni}}$) are fixed although the partial numbers of each kind of atoms (N_{Al}, N_{Ni}) may be changed. The method, as used here, includes four types of trials [17], namely the random move of each atom, the change of identity of an atom selected at random in the simulation box, the site exchange between two atoms of different kinds and the overall volume change of the simulation box. Acceptance is governed by the usual Metropolis algorithm, using the Boltzmann factor appropriate for each kind of trial. The constant external pressure is taken as zero.

The achievement of the equilibrium state is judged by controlling the evolution of instantaneous quantities as cohesive energy, partial concentrations of atomic species and internal pressure. In the present study, 10^6 macro steps were typically sufficient to reach equilibrium.

Clusters containing from 3000 to 12,000 atoms are modeled this way, and Molecular Dynamics (MD) is used to model their assembling. In its simplest form, the MD technique merely consists in numerically solving a system of coupled Newton equations of motion in the microcanonical (NVE) statistical ensemble for the particles contained in the simulated box [20] to which periodic boundary conditions are applied. In systems like nanostructured materials, characterized by large inhomogeneities, this constant volume method is not quite convenient, and one needs to account for the dynamics of the macroscopic deformation of the simulation box, at constant external pressure and temperature. This can be achieved in the canonical ensemble, according to the constrained MD scheme introduced by Rahman and Parinello (RP–MD) [22,23]. In this scheme, the system is extended from $6N$ to $6N + 10$ degrees of freedom. One governs the dynamics of the exchange of energy with an external reservoir at constant temperature [24] and the nine further additional degrees of freedom are the components of three vectors spanning the MD box. The particle Cartesian coordinates as well as these additional degrees of freedom evolve according to equations of motion derived from an appropriate Lagrangian [22].

In the present study we only allow orthogonal macroscopic changes of the model box in order to reach consistency with the MMC simulation model used to monitor segregation. The RP–MD method allows one to apply an external hydrostatic pressure as well as any stress by blocking the appropriate

coefficients of the stress tensor. We apply this method to study the mechanical response of the model compacted sample to a uniaxial load at different temperatures. Zero Kelvin temperature simulations were performed using a standard fast quenching method.

3. The cluster assembled sample

3.1. Isolated clusters

In order to model a cluster assembled material, free clusters need to be modeled first. The structural and thermodynamic properties of free $Ni_{1-x}Al_x$ clusters were already studied in Ref. [17] and they are thus only briefly summarized in this section.

Initial clusters of fixed size are prepared in the $L1_2$ phase by cutting spheres of various radii in a bulk single crystal. The cluster sizes considered range from 3000 to 12,000 atoms. It was found in Ref. [17] that the cores of the Ni_3Al clusters remain $L1_2$. This phase can be predicted by MMC simulations for different fixed chemical potential difference values. The dependence of composition on the chemical potential difference is not quite sensitive to the temperature in this range and it is typical of all cluster sizes considered with $n > 200$. In the cluster cores, this dependence is identical to that found in the bulk material, displaying plateau values typical of the stable phases at the expected stoichiometries. The core is, however, surrounded by a disordered shell in which, depending on $\Delta\mu$, Al segregation may take place [17]. The composition is not constant in the shell and, in case of segregation, the Al concentration monotonically increases from 0.25 to a maximal value at the cluster surface determined by the chemical potential difference between the Ni and the Al subsystems. The relative thickness of the disordered shell is not much cluster size dependent as far as the cluster contains more than about 1000 atoms, which is the case in the present study. The maximal overall excess Al which can be reached is of the order of 10%.

3.2. Cluster assembled materials (CAM)

The method to build a CAM sample is described in Ref. [13] and it thus only summarized here, giving the conditions specific to the present work. Cluster sizes for modeling CAM are sampled in a realistic distribution. Whatever the experimental techniques, size distributions are close to follow a log-normal law. Therefore, model CAM are synthesized with clusters having sizes distributed according to a log-normal law as well. The mean number of atoms per cluster is 7000 and the mean cluster diameter is 5.2 nm.

The free clusters prepared at 300 K as described above are then stacked at random in an imaginary orthogonal box, leaving some separation between their surfaces of no more than about one lattice unit. Periodic boundary conditions are applied to this simulation box. Once filled with clusters, it contains about 10^5 atoms. The system is then ready for compaction by means of a RP–MD simulation. An external hydrostatic pressure of 2 GPa is smoothly reached at 300 K by three successive steps. The box is first equilibrated at zero pressure during 50 ps in order to allow interfacial accommodation. A pressure of 1 GPa is then applied for another 40 ps and finally, a pressure of 2 GPa is applied for during 40 ps again. In each intermediate step, 10–20 ps evolution was sufficient to reach thermal equilibrium. No trend for grain coalescence was observed during the compaction procedure and disordered areas are essentially found at the interfaces. By this method, the time to bring the system to 2 GPa and thermal equilibrium is still close to 15 orders of magnitude shorter than a real compaction experiment and slow processes like segregation, are improperly accounted for. This is the reason why a MMC simulation follows the MD compaction, using the same scheme as for free clusters, though applying suitable periodic boundary conditions. This simulation is done at room temperature, letting the system relax to zero pressure. The chemical potential difference between Ni and Al was adjusted in such a way that no segregation took place in the initial free clusters. Repeating the MMC on the compacted sample induced no significant change in the composition of the interfaces. The atomic density of the CAM samples prepared this way, relative to the bulk material, is typically 88% at 2 GPa and room temperature, independently of the segregation state. When relaxing the sample further at 0 K, the zero pressure density decreases by no more than 0.5%.

4. Mechanical deformation

We now turn to the mechanical response of the CAM model material to a uniaxial load and the case of a NI_3Al single crystal is first examined as a reference case. Fig. 1 shows the strain as a function of temperature in the cased of a uniaxial load of 2 GPa applied in the four lowest index crystallographic directions in the $L1_2$ structure, namely, either a $\langle 1\,0\,0\rangle$, $\langle 1\,1\,0\rangle$, $\langle 1\,1\,1\rangle$ or a $\langle 1\,1\,2\rangle$ direction. The strain is an increasing function of temperature. It is much higher when the load is applied in a $\langle 1\,0\,0\rangle$ direction than when applied in the others. According to Fig. 1, it is a factor 2 at 300 K and a factor 3 at 900 K, while the difference in strains in the other direction differ by less than 20%, whatever the temperature. This is remarkable since no simple geometrical

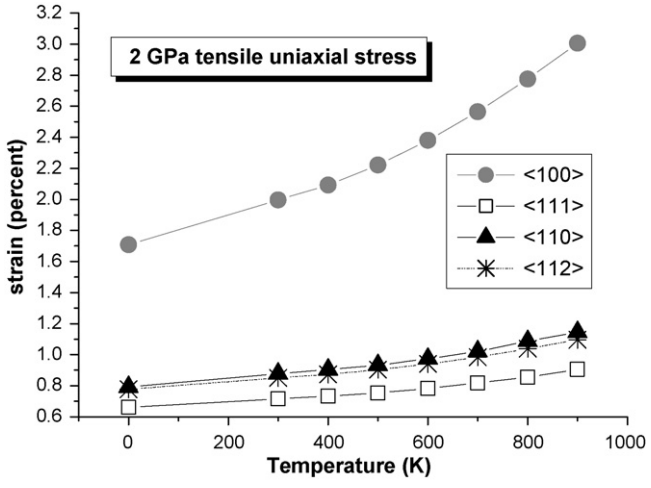

Fig. 1. Strain vs. temperature subsequent to a uniaxial stress of 2 GPa in several low index directions of a Ni_3Al single crystal.

Table 1
Young modulus (E) and Poisson ratio (m) calculated in a Ni_3Al single crystal for ⟨1 0 0⟩ and ⟨1 1 1⟩ uniaxial loads and for compacted Ni_3Al nanostructured samples (CAM) at different temperatures

Material	Direction of load	Temperature (K)	E (GPa)	m[a]
Ni_3Al single crystal	⟨1 1 1⟩	0	276	0.22
	⟨1 0 0⟩	0	100.4	0.38
	⟨1 0 0⟩	300	89.3	0.39
		600	73.7	0.39
		900	61.4	0.39
CAM		0	65.6	0.24–0.28
		300	46.8	0.25–0.45
		600	42.1	0.44–1.04

The experimental values of the Young modulus and Poisson ratio for polycrystalline Ni_3Al are $E_{exp} = 200$ GPa and $m_{exp} = 0.4$ [25].
[a] These values of Poisson ratio m correspond to small uniaxial load region within m values are constant.

consideration explains this difference. The direction dependence of the mechanical response to a stress in single crystals has the consequence of a direction dependent Young modulus. The Young modulus, directly deduced from a strain stress curve is thus also direction dependent. The extension of the simulation box in the direction of the load is accompanied by a transverse size reduction and an associated Poisson ratio can be derived. Because {1 1 1} planes are more compact than {1 0 0}, contractions are of smaller magnitude and the Poisson ratio is smaller too. The values of the Young modulus and the Poisson ratio are given in Table 1, at different temperatures from 0 to 900 K for both directions of the applied load. The experimental values of the Young modulus and of the Poisson ratio for polycrystalline Ni_3Al [25] are within the values predicted with the present potential model for loads applied in the ⟨1 1 1⟩ and ⟨1 0 0⟩ directions of a single crystal. The Poisson ratio is not significantly temperature dependent. Since plastic deformations are hardly induced in perfect infinite single crystals, the same results are expected on a large range of loads, which were checked for loads up to 15 GPa.

The situation is quite different in the CAM sample, which clearly comes out Fig. 2. In this figure, the strain is represented as a function of time at 0–600 K, resulting from different applied loads ranging from 0.1 to 4 GPa. At the lowest stresses considered, the strain quickly becomes constant, which is typical of elastics deformations. Comparing Fig. 2a and b shows that the magnitude of this elastic deformation is not much temperature dependent. This is consistent with the results obtained in a single crystal for load directions different from ⟨1 0 0⟩. When the load is increased, however, strain becomes an increasing function of time. This positive slope increases with load and, as seen by comparing Fig. 2a and b, the dependence of the slope on load is temperature dependent. For instance, at 0 K, the deformation is still elastic under a load of 1.5 Gpa while at 600 K, the increase of strain is so fast that in could not be measured beyond 30 ps. This behavior is characteristic of plastic ongoing deformations, which is confirmed in Fig. 3. In the simulation shown in this figure, a load of 1.2 GPa is applied at 600 K during 100 ps and is then released, letting the CAM evolve freely at constant temperature and zero pressure for another 100 ps. The case of a load of 1.2 GPa is compared to that of a smaller load, namely 0.2 GPa. In the latter case, after releasing the load, the strain reduces to zero, which demonstrates that the deformation induced by the

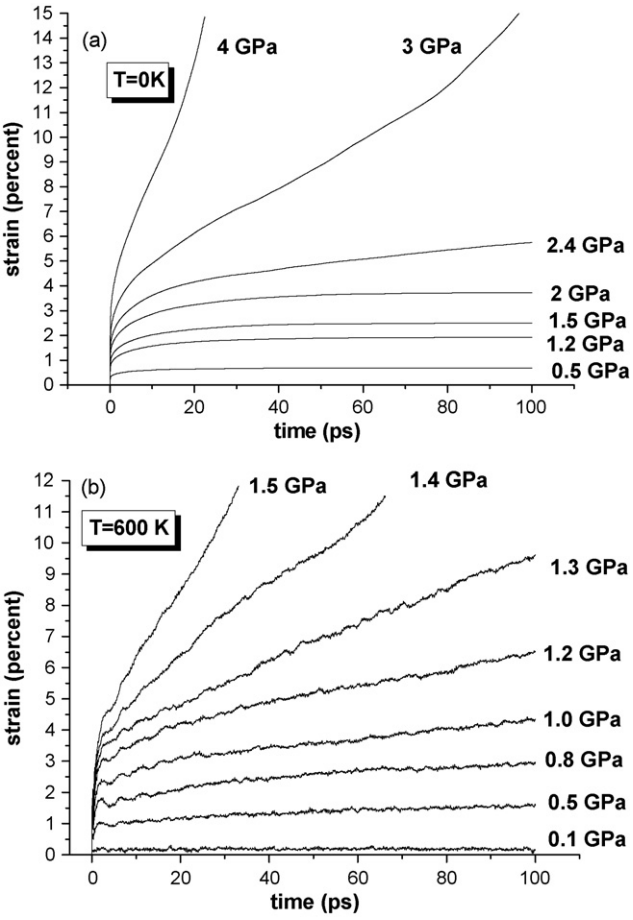

Fig. 2. Strain of the CAM as a function of time in the case of uniaxial loads ranging from 0.1 to 4 GPa. (a) $T = 0$ K and (b) $T = 600$ K.

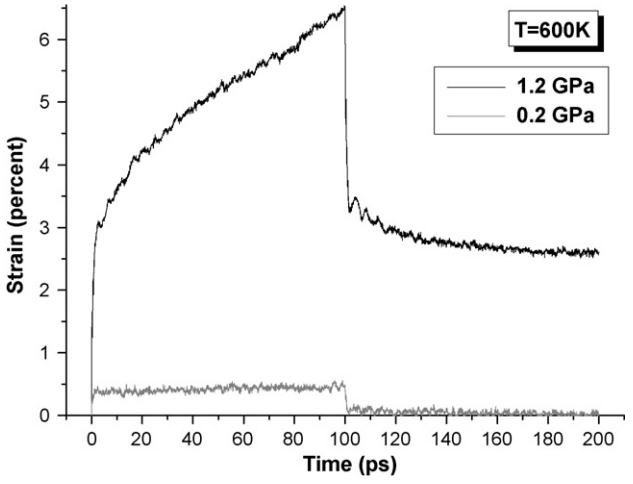

Fig. 3. Time evolution of the strain in the CAM sample at 600 K. A uniaxial load is applied during the 100 ps evolution and is then released, letting the sample freely evolve during another 100 ps. The difference between the effects of elastic and plastic deformations is clearly seen.

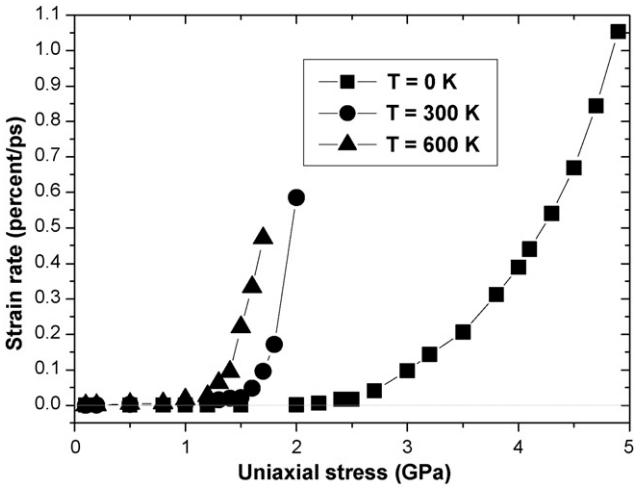

Fig. 4. Strain rate in the CAM as a function of the uniaxial stress at three temperatures.

load is elastic. In the former, the strain reduces as well, but to an intermediate value which can clearly be predicted well above zero at the limit of long times. This is the signature of a plastic deformation. The transition between the elastic and the plastic regimes is illustrated in Fig. 4 where the strain rate is represented as a function of load. At each temperature considered, the strain rate is zero for low load values. A transition is seen to a regime where the strain rate increases with increasing load, corresponding to plastic deformation. An elastic limit can be evidenced at this transition. However, since the transition is smooth, especially at low temperature, the elastic limit is not accurate. It is however, clearly seen higher at 0 K than at 300 and 600 K, and to monotonically decrease with increasing temperature.

In the elastic regime, the same measures as in the case of a single crystal can be performed, and a Young modulus and a Poisson ratio are estimated at the various temperatures considered, except 900 K which is high enough for the CAM sample to start melting. The results are given in Table 1. The Young modulus is clearly below the values obtained with loads applied in low index crystallographic directions, and the experimental estimate for a polycrystal. This is probably the consequence of the occurrence of a large interfacial volume in the nanostructure which contributes to the elastic deformation differently from crystalline areas. The Poisson ratio could only be estimated with limited accuracy and limiting values are given in Table 1. Despite of the inaccuracy, significant temperature dependence is observed, which is also different from the single crystal case and may again be assigned to the role of interfacial areas.

One important mechanism for CAM plastic deformation has been recognized as grain gliding [3]. Here, we have evidence for another one. Indeed, the effect of the load is systematically to decrease the density of the CAM. In the elastic regime, this decrease is never more than 0.1%. In the plastic regime, the density is monotonically decreasing with time and it may reduce by two orders of magnitude more in the range of deformation investigated. This is an indication that deformation proceeds by enlarging the open volumes, which would not occur if grain gliding was the only mechanism involved.

5. Conclusion

The mechanical response of a nanostructured alloy to a uniaxial load is here characterized by means of atomic scale modeling, taking the case of a single crystal as a reference. To our knowledge, no such response has ever been measured for Ni_3Al single crystals, but the Young modulus measured for polycrystalline Ni_3Al falls within the values calculated for a single crystal in various crystallographic directions. As a consequence of the occurrence of large open volumes, the CAM density, after compaction at 2 GPa is more than 10% lower than the density of the single crystal. These volumes induce large differences in the mechanical properties of the material and their temperature dependence. Plastic deformation is evidenced, although the time scale used in the MD simulations is too short for allowing substantial atomic diffusion, nor cluster coalescence. Hence, the plastic deformation observed is not governed by thermal diffusion. On the other hand, the grain size in the CAM is probably too small for allowing a substantial dislocation activity. It is thus most likely that the open volumes play an important role in the plastic behavior and evidence is given therefore, by the decrease of the sample density as its deformation proceeds. Since the size of open volumes depends on the synthesis method, the mechanical properties should depend on them as well.

A previous study showed that interfaces in similar nanostructured materials display some similarities with liquids [4,5] and this suggests the relevance of low friction forces between grains in plastic deformations as well. The further identification of the atomic scale deformation mechanisms is in progress.

Acknowledgements

This work is achieved in the frame of the Belgian network IAP 5-1 “Quantum Size Effect in Nanostructured Materials”. One of us (EZ) acknowledges a research grant of the Belgian National Science Foundation under contract F.R.F.C. 2.4520.03F.

References

[1] K. Lu, H.Y. Zhang, J. Fecht, J. Mater. Res. 12 (4) (1997) 923.
[2] Z. Budrovic, H. Van Swygenhoven, P.M. Derlet, S. Van Petegem, B. Schmitt, Science 304 (2004) 273.
[3] H. Van Swygenhoven, A. Caro, Appl. Phys. Lett. 71 (1997) 1652.
[4] P. Moskovkin, M. Hou, Eur. Phys. J. D27 (2003) 231.
[5] P. Moskovkin, M. Hou, Appl. Surf. Sci. 226 (2004) 161.
[6] H. Van Swygenhoven, A. Caro, Phys. Rev. B 58 (1998) 11246.
[7] P.M. Derlet, H. Van Swygenhoven, Philos. Mag. 82 (2002) 1.
[8] H. Van Swygenhoven, M. Spaczer, A. Caro, Acta mater. 47 (1999) 3117.
[9] G.W. Nieman, J.R. Weertman, R.W. Siegel, Scr. Metall. 23 (1989) 2013.
[10] P. Mélinon, V. Paillard, V. Dupuis, A. Perez, P. Jensen, A. Hoareau, J.P. Perez, J. Tuaillon, M. Broyer, J.L. Vialle, M. Pellarin, B. Baguenard, J. Lerme, Int. J. Mod. Phys. B139 (1995) 339.
[11] L. Bardotti, B. Prevel, P. Melinon, A. Perez, Q. Hou, M. Hou, Phys. Rev. B62 (2000) 2835.
[12] Q. Hou, M. Hou, L. Bardotti, B. Prevel, P. Mélinon, A. Perez, Phys. Rev. B62 (2000) 2825.
[13] M. Hou, V.S. Kharlamov, E.E. Zhurkin, Phys. Rev. B66 (2002) 195408–195411.
[14] V.S. Kharlamov, E.E. Zhurkin, M. Hou, Nucl. Instrum. Methods. B193 (2002) 538.
[15] G.J. Ackland, V. Vitek, Phys. Rev. 41 (15) (1990) 10324.

[16] G.J. Ackland, V. Vitek, Mater. Res. Soc. Symp. Proc. 133 (1989) 105.
[17] E.E. Zhurkin, M. Hou, J. Phys. C12 (2000) 6735.
[18] M.El. Azzaoui, M. Hou, J. Phys. C7 (1996) 6833.
[19] F. Gao, D. Bacon, G. Ackland, Philos. Mag. A 67 (2) (1993) 275.
[20] P. Allen, D. Tildesley, Computer Simulation of Liquids, Clarendon Press, Oxford, 1987.
[21] S.M. Foiles, Phys. Rev. B32 (1985) 7685.
[22] M. Parinello, A. Rahman, Phys. Rev. Lett. 45 (1980) 1196.
[23] M. Parinello, A. Rahman, J. Appl. Phys. 52 (1981) 7182.
[24] S. Nosé, J. Chem. Phys. 81 (1984) 511.
[25] H. Yasuda, T. Takasugi, M. Koiwa, Acta Metall. Mater. 40 (1992) 381.